

## Simulation of Methane Mass Transfer in a Bubble Column: Incipient Turbulent Regime using COMSOL Multiphysics®

Carmen De Crescenzo<sup>a</sup>, Simona Sabbarese<sup>a\*</sup>, Renato Ciampa<sup>b</sup>, Giuseppe Capece<sup>c</sup>, Antimo Migliaccio<sup>a</sup>, Despina Karatza<sup>a</sup>, Simeone Chianese<sup>a</sup>, Dino Musmarra<sup>a</sup>

<sup>a</sup>Department of Engineering, University of Campania Luigi Vanvitelli, Via Roma 29, 81031, Aversa (CE), Italy

<sup>b</sup>Centro Diagnostico Baronia S.r.l., Località Taverna Annibale SNC, Area PIP, Lotto n°7, 83040, Frigento (AV), Italy

<sup>c</sup>Progest S.r.l., Zona ASI Aversa-Nord, Via della Stazione s.n.c., 81030, Gricignano d'Aversa (CE), Italy.

[simona.sabbarese@unicampania.it](mailto:simona.sabbarese@unicampania.it)

Bubble column reactors basically consist of a vertical cylinder filled by a liquid phase in which a gas phase is distributed in the liquid at the column bottom by an appropriate distributor system and moves along the column in the form of bubbles. The aim of a bubble column is to control the rate of mass transfer and reaction between the phases. The liquid phase is modelled as a continuous phase and can be operated in batch mode, or it may move co-currently or counter-currently to the flow of the gas phase. Two-phase and slurry bubble columns are widely used in the chemical- and biochemical industry for carrying out gas-liquid and gas-liquid-solid (catalytic) reaction; in particular, they are used for microalgae growth, aerobic fermentations processes, aerobic treatment of small quantities of highly polluted effluents, as well as oxidation, hydrogenation, chlorination, chemical gas cleaning and, also various biotechnological applications. In this paper, the mass transfer of CH<sub>4</sub> to liquid in a bubble column was investigated by means of Computational Fluid Dynamic simulations in a turbulent regime. The effects of the variation of the most significant fluid dynamic parameters, such as inlet gas velocity, on CH<sub>4</sub> concentration in the liquid phase and mass transfer from gas to liquid were studied by using COMSOL Multiphysics® Modeling Software. Results point out that the higher inlet velocities, the higher the mass transfer rate, which trend shows a pick after which it reduces to zero when CH<sub>4</sub> concentration in the liquid becomes equal to saturation one.

### 1. Introduction

Bubble columns are vertical reactors with a gas distribution system at the bottom, which feeds gas in the form of bubbles in a liquid phase (Musmarra et al., 1992). They are widely used in many chemical and biochemical processes due to their numerous advantages such as good heat and mass transfer, no moving parts, ease of operation, and low operating and maintenance costs (Karatza et al., 2010; Prisciandaro et al., 2009; Sanchez-Forero et al., 2013). In the last years, many studies were based on the use of computational fluid dynamics (CFD) for modelling gas-liquid flows and mass transfer (Becker et al., 1994; Mudde and Simonin, 1999). CFD simulations make it possible to describe the fluid dynamics, the ongoing interactions, the reactive mass transfer, as well as to understand processes occurring in bubble columns (Mühlbauer et al., 2019). Two main approaches have been used to simulate the flow in bubble columns: (i) the Euler–Lagrange approach, in which the fluid flow properties are determined by tracking the motion and properties of the particles as a function of time; (ii) the Euler–Euler approach, in which the fluid properties are expressed as functions of space and time. The choice between the two approaches defines the physical model representative of the gas-liquid interactions (Gemello, 2018). The turbulence is a key element in CFD simulations, which improves heat and mass transfer rates. Different approaches can be used for turbulence modelling: i.e.  $k-\epsilon$ , Realisable  $k-\epsilon$ , Algebraic  $yPlus$ ,  $L-VEL$ ,  $k-\omega$ , SST, Low Reynolds number  $k-\omega$ , Spalart Allmaras e  $v2-f$  (CFD Module COMSOL User's Guide, 2019). The mass transfer of gas into the liquid medium is one of the fundamental parameters to evaluate the reactor performance (Chaumat et al., 2005). According to the two-film theory, the

amount of gas transferred is proportional, through the mass transfer coefficient  $k_L$ , to the concentration gradient and the interfacial area,  $a$  (Garcia-Ochoa and Gomez, 2005). Methane is a cheap substrate, widely available not only as natural gases but also as biogas (Rahnama et al., 2012). It can be used for the production of biopolymers by methanotrophic bacteria, and its utilisation by bacteria for the production of biopolymers in bubble column bioreactors is widely experimentally demonstrated (García-Pérez et al., 2018; Rodríguez et al., 2020); however, the production of biopolymer at large scales requires modelling and numerical simulations (Levett et al., 2016). In this work, the modelling of the mass transfer of methane ( $\text{CH}_4$ ), as gas phase, in water, as liquid phase, was carried out by using the COMSOL Multiphysics® Modeling Software, in which Euler-Euler approach in bubbly flow physics and turbulence  $k$ - $\epsilon$  model were implemented. The dynamic of the mass transfer was investigated by varying two parameters: (i) holes number of the inlet section (1 or 10 holes with 0.003 m diameter) and (ii) inlet gas velocities  $v_{in}$  (0.3, 0.5 and 0.7 m/s).

## 2. Models and methods

### 2.1 Equations of the governing model

The bubbly flow model with two phases (methane gas in liquid water), according to which momentum, continuity, and energy equations are solved for each computational step, was used for the modelling (CFD Module COMSOL User 's Guide, 2019). The turbulence model used is  $k$ - $\epsilon$  coupled with bubble-induced turbulence.

The equation of motion is reported in the following:

$$\phi_l \rho_l \frac{\partial u_l}{\partial t} + \phi_l \rho_l u_l \cdot \nabla u_l = -\nabla p + \nabla \cdot \left[ \phi_l (\mu_l + \mu_T) (\nabla u_l + \nabla u_l^T - \frac{2}{3} (\nabla u_l) I) \right] + \phi_l \rho_l g + F \quad (1)$$

where

- $u_l$  is the velocity vector (SI unit: m/s)
- $p$  is the pressure (SI unit: Pa)
- $\phi$  is the phase volume fraction (SI unit:  $\text{m}^3/\text{m}^3$ )
- $\rho$  is the density (SI unit:  $\text{kg}/\text{m}^3$ )
- $g$  is the gravity vector (SI unit:  $\text{m}/\text{s}^2$ )
- $F$  is any additional volume force (SI unit:  $\text{N}/\text{m}^3$ )
- $\mu_l$  is the dynamic viscosity of the liquid (SI unit:  $\text{Pa}\cdot\text{s}$ ), and
- $\mu_T$  is the turbulent viscosity (SI unit:  $\text{Pa}\cdot\text{s}$ )

The subscripts "l" and "g" denote quantities related to the liquid phase and the gas phase, respectively.

The continuity equation (Equation 2) and the gas phase transport equation (Equation 3) are reported below:

$$\frac{\partial}{\partial t} (\rho_l \phi_l + \rho_g \phi_g) + \nabla \cdot (\rho_l \phi_l u_l + \rho_g \phi_g u_g) = 0 \quad (2)$$

$$\frac{\partial (\rho_g \phi_g)}{\partial t} + \nabla \cdot (\rho_g \phi_g u_g) = -m_{gl} \quad (3)$$

where  $m_{gl}$  is the mass transfer rate from the gas to the liquid (SI unit:  $\text{kg}/(\text{m}^3\cdot\text{s})$ ). The mass transfer rate from the gas to the liquid  $m_{gl}$  is modelled according to the two-film theory (CFD Module COMSOL User 's Guide, 2019):

$$m_{gl} = k_L (c^* - c) M a \quad (4)$$

where  $k_L$  is the mass transfer coefficient (SI unit: m/s),  $c$  is the dissolved gas concentration in liquid (SI unit:  $\text{mol}/\text{m}^3$ ),  $M$  is molecular weight of species (SI unit:  $\text{kg}/\text{mol}$ ),  $a$  is the interfacial area per volume (SI unit:  $\text{m}^2/\text{m}^3$ ); while Henry's law allows calculating the equilibrium concentration  $c^*$  of gas dissolved in liquid:

$$c^* = \frac{p + p_{ref}}{H} \quad (5)$$

where  $H$  is Henry's constant and  $p_{ref}$  reference pressure (SI unit: Pa) (CFD Module COMSOL User 's Guide, 2019). For the two-film theory, the concentration of the dissolved gas needs to be calculated by adding a Transport of Diluted Species interface by means of the solution of the following equation:

$$\frac{\partial c}{\partial t} + \nabla \cdot (c u_l) = \nabla \cdot (D \nabla c) + \frac{m_{gl}}{M} \quad (6)$$

The interfacial area  $a$  (SI unit:  $\text{m}^2/\text{m}^3$ ) can be calculated by using the number density,  $n$ , and the volume fraction of gas per unit volume,  $\phi_g$  (CFD Module COMSOL User 's Guide, 2019):

$$a = (4n\pi)^{\frac{1}{3}} (3\phi_g)^{2/3} \quad (7)$$

The Mass transfer coefficient  $k_L$  is an input data of the model and was calculated by using the typical approach based on Sherwood number,  $Sh$ , diffusivity of gas in liquid,  $D_{gas,liquid}$  (SI unit:  $\text{m}^2/\text{s}$ ), and bubble diameter  $d_b$  (SI unit: m):

$$k_L = \frac{Sh D_{gas,liquid}}{d_b} \quad (8)$$

Sherwood number Sh for rising large bubbles of gas in liquid as continuous phase ( $d_b > 2$  mm) was calculated according to Equation 9 (Calderbank et al., 1970):

$$Sh = 1.13 Sc^{1/2} Re^{1/2} \quad (9)$$

Where Sc and Re represent Schmidt and Reynolds non-dimensional numbers and were calculated from Equations 10 and 11, respectively (Perry et al., 1997):

$$Sc = \frac{\mu_l}{\rho_l D_{gas,liquid}} \quad (10)$$

$$Re = \frac{d_b \rho_l v_t}{\mu_l} \quad (11)$$

$v_t$  is the terminal velocity of bubble calculated according to the following equation (Bird et al., 2002):

$$v_t = \sqrt{\frac{8 F_D}{C_D \pi d_b^2 \rho_l}} \quad (12)$$

$F_D$  is the drag force calculated according to Equation 13, and  $C_D$  is the Drag coefficient was assumed equal to 0.44 for turbulent flow (Bird et al., 2002):

$$F_D = \frac{\pi d_b^3 g (\rho_l - \rho_g)}{6} \quad (13)$$

## 2.2 Simulation process

The physic-chemical properties, such as density and dynamic viscosity, of methane and water were defined according to the COMSOL Multiphysics® materials' properties database. The geometry of the column was assumed to be rectangular 0.5 m large and 1.5 m high. Geometrical column properties are the same used by several researchers (Becker et al., 1994; Mudde and Simonin, 1999). Inlet of gas phase was modelled as 1 hole with 0.003 m diameter and 10 holes with 0.003 m diameter. Bubble diameter,  $d_b$ , was set equal to the inlet (0.003 m). The problem was solved in two-dimensional geometry and finer free triangular mesh was built in the whole domain. The system temperature was set to 298.15 K. The reference pressure was equal to 101,325 Pa; the pressure in the column was set in the Fluid Properties interface according to the following equation (CFD Module COMSOL User's Guide, 2019):

$$p = (\rho_l \phi_l + \rho_g \phi_g) g (H_{column} - y) \quad (14)$$

where  $y$  is y-axis coordinate [m] and  $H_{column}$  is the column's height (1.5 m). y-axis coordinate is equal to 0 m and 1.5 m at the bottom and the top of the bubble column, respectively. Three gas velocities were investigated: 0.3 m/s, 0.5 m/s, and 0.7 m/s for both inlet configurations (inlet configurations: 1 hole or 10 holes). Table 1 summarises the CH<sub>4</sub> flow rate fed to the bubble column for both the inlet configurations at the inlet velocities investigated, respectively.

Table 1. CH<sub>4</sub> gas flow rate for the investigated inlet configurations

	$v_{in}=0.3$ m/s	$v_{in}=0.5$ m/s	$v_{in}=0.7$ m/s
Inlet holes number	CH <sub>4</sub> Flow rate [m <sup>3</sup> /s]	CH <sub>4</sub> Flow rate [m <sup>3</sup> /s]	CH <sub>4</sub> Flow rate [m <sup>3</sup> /s]
1	$2.12 \times 10^{-5}$	$3.5 \times 10^{-5}$	$4.9 \times 10^{-5}$
10	$2.12 \times 10^{-4}$	$3.5 \times 10^{-4}$	$4.9 \times 10^{-4}$

## 3. Results and discussion

The non-dimensional group Re, Sc, and Sh were equal to 1004, 598 and 876, respectively, highlighting the condition of the incipient turbulence regime. The mass transfer coefficient  $k_L$  value was equal to 0.00044 m/s, which is comparable with the literature values (Reeves, 1988). In Figure 1.a and Figure 1.b dissolved CH<sub>4</sub> concentration in function of the time is showed for 1-hole and 10-holes inlet configurations, respectively, at the column height  $y=1.125$  m. As it can be seen, the higher the inlet velocity, the lower the saturation time for both configurations. CH<sub>4</sub> concentration at saturation is slightly different for the cases investigated because of the different values of pressure in the column, which depend on the gas hold-up. As consequence, the total mass of CH<sub>4</sub> transferred from gas to liquid slightly varies, resulting in  $5.55 \times 10^{-5}$  kg,  $5.50 \times 10^{-5}$  and  $5.49 \times 10^{-5}$  for 1-hole inlet configuration for 0.3, 0.5, and 0.7 m/s inlet velocity, respectively; and  $5.55 \times 10^{-5}$  kg,  $5.53 \times 10^{-5}$  and  $5.39 \times 10^{-5}$  for 10-holes inlet configuration for 0.3, 0.5, and 0.7 m/s inlet velocity, respectively.

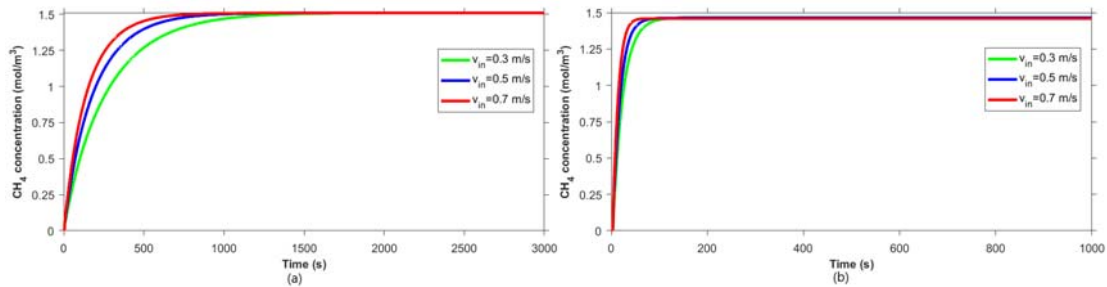


Figure 1. Trends of dissolved  $CH_4$  concentration during simulated experiments at column height  $y=1.125m$ : 1-hole inlet configuration a); 10-holes inlet configuration b)

The time for saturating the column reduced by increasing the inlet gas velocity and by passing from 1-hole inlet to 10 10-holes inlet because of the higher  $CH_4$  flow rate (Table 1). In particular, the saturation times are 1650 s, 1100 s, and 870 s for 1-hole inlet configuration, and 185 s, 175 s, and 135 s for 10-holes inlet configuration, for  $v_{in}$  equal to 0.3, 0.5 and 0.7 m/s, respectively.

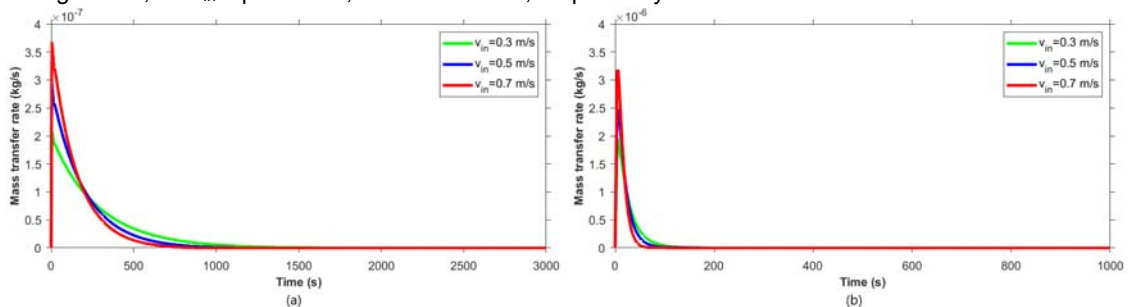


Figure 2.  $CH_4$  mass transfer during simulated experiments: 1-hole inlet configuration a); 10-holes inlet configuration b)

In Figure 2,  $CH_4$  mass transfer rate as a function of time for the investigated inlet velocities is shown for 1-hole (Figure 2.a) and 10-holes (Figure 2.b) inlet configurations. The higher the inlet velocities, the higher the transfer rate; however, for all the velocities investigated, the mass transfer rate achieved a peak, after which it reduced up to zero when  $CH_4$  concentration becomes equal to saturation one. In particular, the mass transfer rate results in the order of magnitude of  $10^{-7}$  kg/s and  $10^{-6}$  kg/s for 1-hole and 10-holes inlet configurations, respectively. This behaviour is related to the greater gas flow rate with the 10-holes inlet configuration, which is ten-time higher than the  $CH_4$  mass transfer rate achieved with the 1-hole inlet configuration. Figure 3 and Figure 5 display the concentration contours of  $CH_4$  in water for 1-hole inlet configuration at 500 and 2000 s (saturation), respectively, at all the velocities investigated; Figure 5 and Figure 6 display the concentration contours of  $CH_4$  in water for the 10-holes inlet configuration at 50 s and 300 s (saturation), respectively. The variation of methane concentration in the liquid phase strongly depends on the inlet configuration, i.e. fluid dynamic conditions. The contours show that the methane concentration reduces by distancing from the inlet holes. With the 10-holes inlet configuration the dispersion of methane was characterised by a stratified distribution, while with 1-hole inlet configuration the dispersion of methane showed a vertical distribution. At saturation, the variation of the methane concentration is related to the variation of gas hold-up and pressure along the column.

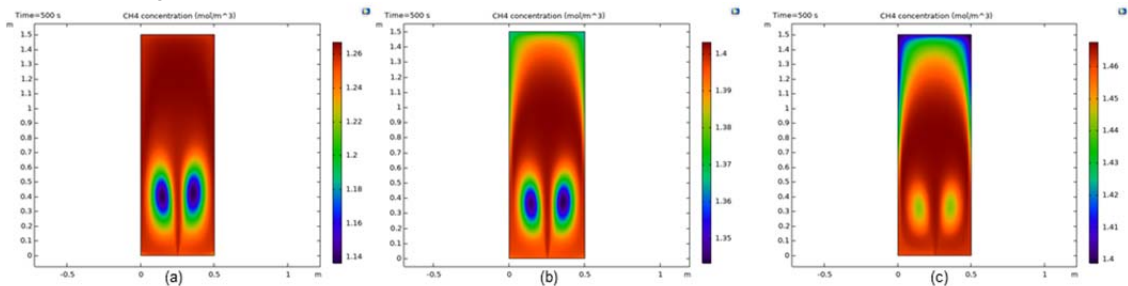


Figure 3. Concentration contours of  $CH_4$  for 1-hole inlet configuration at 500 s at different inlet gas velocities: 0.3 m/s a), 0.5 m/s b), 0.7 m/s c)

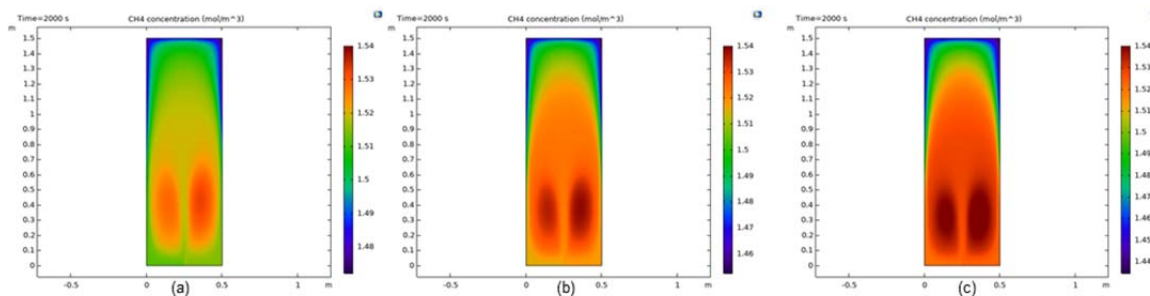


Figure 4. Concentration contours of  $\text{CH}_4$  for 1-hole inlet configuration at 2000 s at different inlet gas velocities: 0.3 m/s a), 0.5 m/s b), 0.7 m/s c)

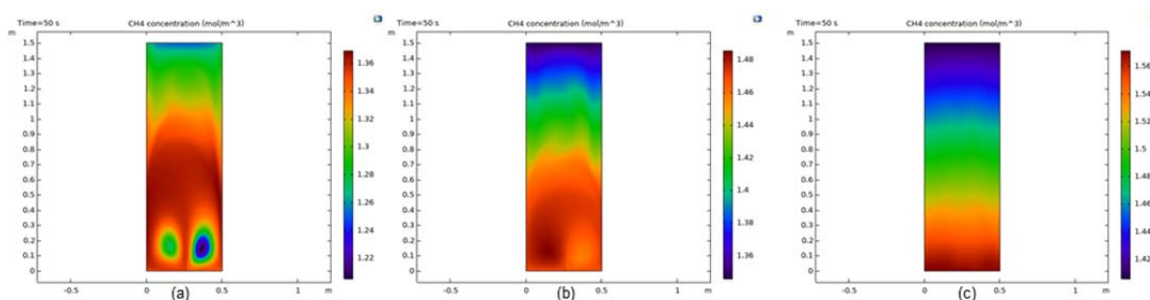


Figure 5. Concentration contours of  $\text{CH}_4$  for 10-holes inlet configuration at 50 s at different inlet gas velocities: 0.3 m/s a), 0.5 m/s b), 0.7 m/s c)

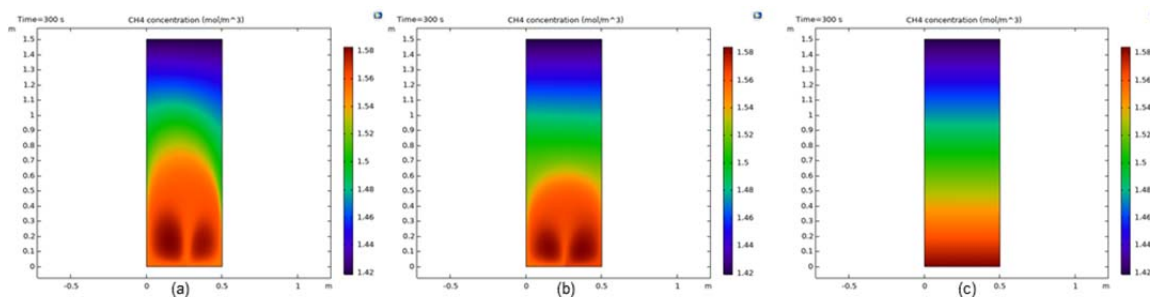


Figure 6. Concentration contours of  $\text{CH}_4$  for 10-holes inlet configuration at 300 s at different inlet gas velocities: 0.3 m/s a), 0.5 m/s b), 0.7 m/s c)

#### 4. Conclusions

The mass transfer of  $\text{CH}_4$  to water in a bubble column at the incipient turbulent regime ( $\text{Re} = 1004$ ) was investigated by varying the inlet gas velocities and the number of the inlet holes of the gas. For the fluid dynamic conditions considered, the mass transfer coefficient value was equal to 0.00044 m/s. The higher the inlet velocities, the lower the time required to saturate the column with methane for both the inlet configurations. Moreover, by keeping constant the inlet velocity, the saturation time reduces by increasing the number of inlet holes, which corresponds to the increase of the methane flow rate. The mass transfer rate increases by increasing the inlet velocities; in particular, the trend of the mass transfer rate is characterised by the achievement of a pick, after which it reduces to zero when  $\text{CH}_4$  concentration in the liquid becomes equal to saturation one. The variation of the methane concentration in the liquid phase is related to the inlet configuration, i.e. the fluid dynamic conditions; in particular, at saturation, the variation of the methane concentration depends on the variation of gas hold-up and pressure along the column.

#### Acknowledgments

This work has been funded by the “Biomasse x Batteri x Bioraffinerie x Biomateriali for Value (Bio44V)” Project, Fondo per la Crescita Sostenibile – Sportello “Agrifood” PON I&C 2014-2020, di cui al D.M. 5 marzo 2018 Capo III. This work has been supported by VALERE “VANviteLli pER la RicERca” PROGRAMME funded by the University of Campania “Luigi Vanvitelli”.

## References

- Becker, S., Sokolichin, A., and Eigenberger, G., 1994, Gas-liquid flow in bubble columns and loop reactors: Part II. Comparison of detailed experiments and flow simulations, *Chemical Engineering Science*, [https://doi.org/10.1016/0009-2509\(94\)00290-8](https://doi.org/10.1016/0009-2509(94)00290-8)
- Bird, R. B., Stewart, W. E., and Lightfoot, E. N., 2002, *Transport phenomena, second edition*
- Calderbank, P. H., Johnson, D. S. L., and Loudons, J., 1970, Mechanics and mass transfer of single bubbles in free rise through some Newtonian and non-Newtonian liquids, *Chemical Engineering Science*, 25, 235–256
- CFD Module COMSOL User's Guide, 2019, *COMSOL Multiphysics*
- Chamat, H., Billet-Duquenne, A. M., Augier, F., Mathieu, C., and Delmas, H., 2005, Mass transfer in bubble column for industrial conditions - Effects of organic medium, gas and liquid flow rates and column design, *Chemical Engineering Science*, 60, 5930–5936, <https://doi.org/10.1016/j.ces.2005.04.026>
- García-Ochoa, F., and Gomez, E., 2005, Prediction of gas-liquid mass transfer coefficient in sparged stirred tank bioreactors, *Biotechnology and Bioengineering*, 92, 761–772, <https://doi.org/10.1002/bit.20638>
- García-Pérez, T., López, J. C., Passos, F., Lebrero, R., Revah, S., and Muñoz, R., 2018, Optimization of CH<sub>4</sub> removal from diluted emissions and continuous PHB production by *Methylocystis hirsuta*: Towards GHG biorefineries, *Chemical Engineering Transactions*, <https://doi.org/10.3303/CET1868074>
- Gemello, L., 2018, Modelling of the hydrodynamics of bubble columns using a two-fluid model coupled with a population balance approach., PhD Thesis in Mechanics of the Fluids
- Karatza, D., Prisciandaro, M., Lancia, A., and Musmarra, D., 2010, Sulfite oxidation catalyzed by cobalt ions in flue gas desulfurization processes, *Journal of the Air and Waste Management Association*, 60, 675–680, <https://doi.org/10.3155/1047-3289.60.6.675>
- Levett, I., Birkett, G., Davies, N., Bell, A., Langford, A., Laycock, B., Lant, P., and Pratt, S., 2016, Techno-economic assessment of poly-3-hydroxybutyrate (PHB) production from methane - The case for thermophilic bioprocessing, *Journal of Environmental Chemical Engineering*, 4, 3724–3733, <https://doi.org/10.1016/j.jece.2016.07.033>
- Mudde, R. F., and Simonin, O., 1999, Two- and three-dimensional simulations of a bubble plume using a two-fluid model, *Chemical Engineering Science*, [https://doi.org/10.1016/S0009-2509\(99\)00234-1](https://doi.org/10.1016/S0009-2509(99)00234-1)
- Mühlbauer, A., Hlawitschka, M. W., and Bart, H. J., 2019, Models for the Numerical Simulation of Bubble Columns: A Review, *Chemie-Ingenieur-Technik*, 91, 1747–1765, <https://doi.org/10.1002/cite.201900109>
- Musmarra, D., Vaccaro, S., Fillai, M., and Massimilla, L., 1992, Propagation characteristics of pressure disturbances originated by gas jets in fluidized beds, *International Journal of Multiphase Flow*, 18, 965–976, [https://doi.org/10.1016/0301-9322\(92\)90070-W](https://doi.org/10.1016/0301-9322(92)90070-W)
- Perry, R. H., Green, D. W., and Maloney, J. O., 1997, *Perry's Chemical Engineer's Handbook*, Seventh Edition In *Society*, <https://doi.org/10.1036/0071422943>
- Prisciandaro, M., Olivieri, E., Lancia, A., and Musmarra, D., 2009, Gypsum Scale Control by Nitrotrimethylenephosphonic Acid, *Industrial & Engineering Chemistry Research*, 48, 10877–10883, <https://doi.org/10.1021/ie900253f>
- Rahnama, F., Vasheghani-Farahani, E., Yazdian, F., and Shojaosadati, S. A., 2012, PHB production by *Methylocystis hirsuta* from natural gas in a bubble column and a vertical loop bioreactor, *Biochemical Engineering Journal*, 65, 51–56, <https://doi.org/10.1016/j.bej.2012.03.014>
- Reeves, P., 1988, Handbook of separation process technology In *TrAC Trends in Analytical Chemistry* (Vol. 7, Issue 7), [https://doi.org/10.1016/0165-9936\(88\)85078-7](https://doi.org/10.1016/0165-9936(88)85078-7)
- Rodríguez, Y., Firmino, P. I. M., Pérez, V., Lebrero, R., and Muñoz, R., 2020, Biogas valorization via continuous polyhydroxybutyrate production by *Methylocystis hirsuta* in a bubble column bioreactor, *Waste Management*, 113, 395–403, <https://doi.org/10.1016/j.wasman.2020.06.009>
- Sanchez-Forero, D. I., Silva, J. L., Silva, M. K., Bastos, J. C. S. C., and Mori, M., 2013, Experimental and numerical investigation of gas-liquid flow in a rectangular bubble column with centralized aeration flow pattern, *Chemical Engineering Transactions*, <https://doi.org/10.33032/CET1332261>